THE JOURNAL OF BIOLOGICAL CHEMISTRY VOL. 287, NO. 44, pp. 37458–37471, October 26, 2012

Differentiation of the DnaA-*oriC* Subcomplex for DNA Unwinding in a Replication Initiation Complex*[S]

Received for publication, April 12, 2012, and in revised form, August 7, 2012 Published, JBC Papers in Press, August 31, 2012, DOI 10.1074/jbc.M112.372052

Shogo Ozaki[1], **Yasunori Noguchi, Yasuhisa Hayashi**[2], **Erika Miyazaki, and Tsutomu Katayama**[3]

From the Department of Molecular Biology, Graduate School of Pharmaceutical Sciences, Kyushu University, 3-1-1 Maidashi, Higashi-ku, Fukuoka 812-8582, Japan

Background: Multiple DnaA molecules form highly ordered complexes on the origin DNA to initiate chromosomal replication.
Results: Novel structural motifs of DnaA are specifically required for the formation of the DNA unwinding-specific DnaA subcomplex.
Conclusion: Distinct inter-DnaA interactions are required for the unwinding-specific subcomplex.
Significance: Differentiation of the unwinding-specific subcomplex and a key mechanism underlying it are revealed.

In *Escherichia coli*, ATP-DnaA multimers formed on the replication origin *oriC* promote duplex unwinding, which leads to helicase loading. Based on a detailed functional analysis of the *oriC* sequence motifs, we previously proposed that the left half of *oriC* forms an ATP-DnaA subcomplex competent for *oriC* unwinding, whereas the right half of *oriC* forms a distinct ATP-DnaA subcomplex that facilitates helicase loading. However, the molecular basis for the functional difference between these ATP-DnaA subcomplexes remains unclear. By analyzing a series of novel DnaA mutants, we found that structurally distinct DnaA multimers form on each half of *oriC*. DnaA AAA+ domain residues Arg-227 and Leu-290 are specifically required for *oriC* unwinding. Notably, these residues are required for the ATP-DnaA-specific structure of DnaA multimers in complex with the left half of *oriC* but not for that with the right half. These results support the idea that the ATP-DnaA multimers formed on *oriC* are not uniform and that they can adopt different conformations. Based on a structural model, we propose that Arg-227 and Leu-290 play a crucial role in inter-ATP-DnaA interaction and are a prerequisite for the formation of unwinding-competent DnaA subcomplexes on the left half of *oriC*. These residues are not required for the interaction with DnaB, nucleotide binding, or regulatory DnaA-ATP hydrolysis, which further supports their important role in inter-DnaA interaction. The corresponding residues are evolutionarily conserved and are required for unwinding in the initial complexes of *Thermotoga maritima*, an ancient hyperthermophile. Therefore, our findings suggest a novel and common mechanism for ATP-DnaA-dependent activation of initial complexes.

In cellular organisms, the unwinding of duplex DNA is a fundamental step during the initiation of chromosomal replication. This reaction requires highly organized nucleoprotein complexes that are formed on the replication origin. In *Escherichia coli*, DnaA multimers in complex with the replication origin *oriC* play key roles in duplex DNA unwinding (1–6). ATP-bound DnaA (ATP-DnaA) molecules form functional multimers on *oriC*, which can unwind duplex DNA within this region, resulting in open complexes (1, 2). Subsequently, DnaB helicase is recruited onto the resultant single-stranded DNA (ssDNA) region via direct interaction with the DnaA-*oriC* complexes and the DnaC helicase loader (7, 8). DnaB helicase extends the ssDNA region and promotes the loading of replication components, including DnaG primase and DNA polymerase III holoenzyme, thereby initiating chromosomal replication (6, 9, 10). After initiation, DnaA-ATP hydrolysis is promoted by the interaction between ADP-Hda protein and the DNA-loaded clamp subunit of DNA polymerase III holoenzyme, which yields initiation-inactive ADP-bound DnaA (ADP-DnaA) (11–15). ADP-DnaA multimers formed on *oriC* are incompetent for duplex DNA unwinding (16). This DnaA-ATP hydrolysis mechanism is termed regulatory inactivation of DnaA (RIDA)[4] and is required for ensuring once-per-cell-cycle initiation by repressing extra initiation events (15, 17–22). For the next round of initiation, ADP-DnaA is reactivated into ATP-DnaA by a nucleotide exchange reaction mediated by DnaA multimers in complex with the DnaA-reactivating sequences on the chromosome (23).

The minimum *oriC* in *E. coli* consists of an AT-rich duplex unwinding element (DUE) and a flanking DnaA assembly region (DAR) (Fig. 1) (1–5). DAR is crucial for the nucleoprotein complex formation and includes multiple DnaA-binding sites, which are termed R1–R5, I1–I3, τ1 and τ2, and C1–C3

* This work was supported by Grants-in-aid from the Ministry of Education, Culture, Sports, Science, and Technology of Japan and the Japan Society for Promotion of Science (Grants 19370077, 17080005, and 21770187).
[S] This article contains supplemental Table 1 and Figs. 1 and 2.
[1] Present address: Biozentrum, University of Basel, CH-4056 Basel, Switzerland.
[2] Present address: Chemo-Sero-Therapeutic Research Institute, Kumamoto 860-8568, Japan.
[3] To whom correspondence should be addressed. Tel.: 81-92-642-6641; Fax: 81-92-642-6646; E-mail: katayama@phar.kyushu-u.ac.jp.

[4] The abbreviations used are: RIDA, regulatory inactivation of DnaA; DUE, duplex unwinding element; ssDUE, single-stranded DUE; dsR1, double-stranded R1; DAR, DnaA assembly region; AAA, ATPases associated with a variety of cellular activities; DF, DUE-flanking; LL, left low affinity; RL, right low affinity; RE, right edge; AID, ATP-DnaA-specific interactive locus for DUE unwinding; ss-dsDUE, single-stranded DUE conjugated to double-stranded DNA.

(1–5, 24–26). DnaA-binding sites R1 and R4 at both edges of DAR have the highest affinity for both ATP- and ADP-DnaA (27). A moderate affinity site (R2) and low affinity sites (R5, I1–I3, τ1 and τ2, and C1–C3) located between R1 and R4 preferentially bind ATP-DnaA oligomers rather than ADP-DnaA (Fig. 1) (5, 22, 24, 25, 28, 29). C1–C3 sites were recently proposed to be low affinity DnaA-binding sites (26). Independent footprint data are consistent with C2 and C3 sites rather than DnaA-binding site R3, which overlaps with the C2 and C3 sites and has been proposed to be a member of the low affinity sites (Fig. 1) (24, 26).

The resulting ATP-DnaA-DAR complexes unwind DUE, which results in an open complex. The T-rich strand but not the A-rich strand of the unwound ssDUE binds to ATP-DnaA-DAR complexes and stabilizes the open complex, which is required for DnaB helicase loading onto the A-rich strand (29–32). DAR contains a binding site for IHF, a nucleoid-associated protein that induces sharp (~180°) DNA bending (Fig. 1) (33). IHF binding to this site stimulates replication initiation both *in vitro* and *in vivo* (34–37). This is consistent with the fact that IHF stimulates the interaction between ssDUE and ATP-DnaA-DAR complexes (31) (Fig. 1). An alternative model where ATP-DnaA molecules bind to ssDUE, resulting in a continuous multimer covering the region from ssDUE to DAR, has also been proposed (38–40). However, ATP-DnaA binding to ssDUE in the absence of DAR requires much higher concentrations of DnaA than the binding of ssDUE to ATP-DnaA-DAR complexes (29, 31).

E. coli DnaA consists of four functional domains (Fig. 1) (2, 4, 6). Domain I interacts with several proteins, including DnaB, DiaA, and the DnaA domain I within another protomer in DnaA complexes (41–43). DiaA stimulates ATP-DnaA assembly, especially on the ATP-DnaA-preferential low affinity sites, by binding to multiple DnaA molecules (28). Domain II is a flexible linker (43, 44). Domain III contains motifs characteristic of the AAA+ family (*e.g.* Walker A/B, sensor 1/2, and an Arg finger) and plays a crucial role in ATP/ADP binding/hydrolysis, inter-DnaA interaction, and DUE unwinding (4, 45, 46). Domain IV has a DNA-binding helix-turn-helix motif (46, 47), in addition to an amphiphilic helix, which is connected to domain III and might be important for inter-DnaA interaction (48).

Similar to typical AAA+ proteins, the ATP-DnaA multimer on *oriC* is thought to adopt a spiral structure containing a central pore (Fig. 1) (29, 49). In this complex, the DnaA AAA+ domain Arg finger (Arg-285) is required for the cooperative binding of ATP-DnaA molecules to moderate and low affinity DnaA-binding sites within DAR (24). This motif is thought to interact with ATP bound to the adjacent protomer within ATP-DnaA-*oriC* complexes, thereby promoting cooperative binding and the overall formation of ATP-DnaA multimers on DAR, which is required for open complex formation (24). In addition, B/H motifs (Val-211 and Arg-245) in the DnaA AAA+ domain are specifically required for ssDUE binding in open complexes (29). In the proposed DnaA spiral, each of these protomer motifs is regularly projected onto the pore surface, which probably supports direct and stable binding to ssDUE (4, 29, 40) (Fig. 1).

We recently found that DnaA-DAR complexes consist of functionally distinct DnaA subcomplexes that assemble on distinct DAR regions (*i.e.* the DUE-flanking (DF), left low affinity (LL), right low affinity (RL), and right edge (RE) regions (Fig. 1) (31). The DF region carries the high affinity DnaA box R1, and the LL region carries the low affinity binding sites (*i.e.* R5, I1 and I2, and τ1 and τ2). The ATP-DnaA multimer in complex with the LL region is competent for ssDUE binding, which is facilitated by the DnaA-DF subcomplex, and thereby sustains DUE unwinding and open complex formation. These DUE unwinding processes are drastically enhanced by IHF binding to its binding site. The IHF-mediated DNA bending is inferred to promote the interaction between the DF-DnaA and LL-DnaA subcomplexes, which then stimulates the binding of ssDUE to the LL-DnaA subcomplex (Fig. 1). This stimulation mechanism in DUE unwinding is referred to as ssDUE recruitment. In contrast, the DnaA multimer formed on the RL-RE regions is not required for DUE unwinding but stimulates interaction with DnaB and its loading onto ssDUE. Thus, the DnaA multimers formed on the LL and RL-RE regions are functionally distinct (31). However, structural evidence supporting these functional differences in DnaA multimers is still lacking.

In the current study, we analyzed a series of DnaA AAA+ domain residues that were predicted to be important for the inter-DnaA interaction based on homology modeling. Further analyses revealed that *E. coli* DnaA Arg-227 and Leu-290 residues were crucial for DUE unwinding and ssDUE binding. Notably, these residues were required for binding to the ATP-DnaA-preferential low affinity sites within the LL region but not those within the RL-RE regions. Rather than being uniform in overall structure, these results indicate that DnaA multimers formed on LL and RL-RE regions adopt structurally different inter-DnaA interaction modes, which may explain the functional difference between DnaA multimers. Also, these residues are evolutionarily conserved, and the corresponding mutants of the DnaA ortholog (*tma*DnaA) from the ancient hyperthermophile *Thermotoga maritima* are inactive in DUE unwinding of its cognate *oriC* (*tma-oriC*). Based on these results, our findings suggest a novel and common mechanism for ATP-DnaA-dependent activation of initial complexes.

EXPERIMENTAL PROCEDURES

Strains—*E. coli* strains KH5402–1 (wild type (WT)), KA413 (KH5402-1 *dnaA46 ilv*$^+$), and KA451 (KH5402-1 *dnaA*::Tn*10 rnhA*::*cat*) were described previously (23).

Buffers—Buffer N′ was composed of 50 mM Hepes-KOH (pH 7.6 at 1 M), 0.3 mM EDTA, 7 mM dithiothreitol, 20% (v/v) glycerol, and 0.007% Triton X-100. Buffer N was the same as buffer N′, except with the addition of 2.5 mM magnesium. Buffer P comprised 60 mM Hepes-KOH (pH 7.6), 0.1 mM zinc acetate, 8 mM magnesium acetate, 30% (v/v) glycerol, 0.32 mg/ml bovine serum albumin, and 5 mM ATP. Buffer G′ consisted of 20 mM Hepes-KOH (pH 7.6), 1 mM EDTA (pH 8.0), 4 mM dithiothreitol, 5 mM magnesium acetate, 10% (v/v) glycerol, 1 mM ATP, and 0.1% Triton X-100. Buffer G was the same as buffer G′, except with the addition of 0.1 mg/ml bovine serum albumin and 50 mM ammonium sulfate. Buffer F included 25 mM Hepes-KOH (pH 7.6), 5 mM calcium acetate, 2.8 mM magnesium ace-

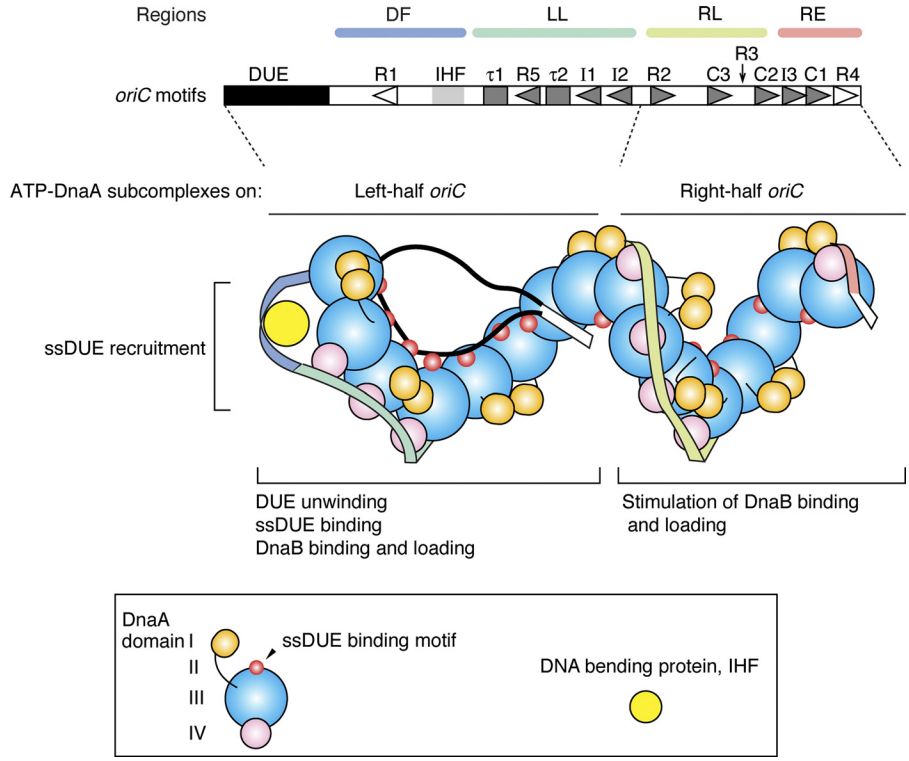

FIGURE 1. **Model of an open complex and basic structures of *E. coli oriC* and DnaA.** *E. coli oriC* consists of DUE, which has AT-rich repeats, and DAR, which carries an IHF binding site (*light gray*) and multiple DnaA-binding sites (*i.e.* R, I, τ, and C sites; *open* or *dark gray symbols*). The *arrowheads* indicate the orientation of R, I, and C sites. The highest affinity sites, R1 and R4, are indicated by *open symbols*. DAR can be divided into four functional regions (*i.e.* DF, LL, RL, and RE). *E. coli* DnaA domains (I, II, III, and IV) and IHF are also shown in *different colors*. The ATP-DnaA multimer formed on DAR binds ssDUE (*heavy lines*). The binding of ssDUE to the ATP-DnaA multimer formed on LL region is stimulated by IHF (*yellow*) and the DF (DnaA box R1)-bound ATP-DnaA. This stimulation is probably caused by the sharp DNA bending induced by IHF and the interaction between the DF-bound ATP-DnaA and the LL-bound ATP-DnaA multimer (*i.e.* ssDUE recruitment), as illustrated in Ref. 31.

tate, 45 mM ammonium sulfate, 4 mM dithiothreitol, 10% (v/v) glycerol, 0.2% Triton X-100, 0.5 mg/ml bovine serum albumin, 14 μg/ml poly(dA-dT)-(dA-dT), and 14 μg/ml poly(dI-dC)-(dI-dC). Buffer R contained 20 mM Tris-HCl (pH 7.5), 10% glycerol, 8 mM dithiothreitol, 0.01% Brij-58, 8 mM magnesium acetate, 120 mM potassium glutamate, and 0.1 mg/ml bovine serum albumin. Buffer GS contained 20 mM Hepes-KOH (pH 8.0), 5 mM magnesium acetate, 1 mM EDTA, 4 mM dithiothreitol, 0.2% Triton X-100, 5% (v/v) glycerol, 0.5 mg/ml bovine serum albumin, 2 mM ATP, and 60 mM KCl.

DNA and Proteins—pBSoriC, M13KEW101, pKA234, pING1, pRNHH, pOZ18, pTHMA-1, and pOZ14 were described previously (29, 31, 42, 50). Plasmids used for the overexpression of mutant DnaA and *tma*DnaA proteins were derivatives of pKA234 and pTHMA-1, respectively. These plasmids were constructed using a QuikChange site-directed mutagenesis kit (Stratagene) and mutagenic primers (see supplemental Table 1). A pOZ18 derivative pmF239A bearing the *dnaA F239A* allele was constructed as described previously (51). ssDUE-dsR1 and ssDUE-dsNon are the same as ssDUE-R1 and ssDUE-non, respectively, both of which were described previously (31). The *oriC* fragment for DNase I footprint experiments; the biotinylated *oriC* DNA for the pull-down assay; and DARΔR1 DNA, which is a DAR fragment lacking DnaA-binding site R1, were also described previously (28, 29, 31). For analysis of *oriC* subcomplexes, the RL-RE DNA (122 bp) was prepared by PCR using pBSoriC and primers oriR2R4 and ori2. Primer ori2 and the DF-LL (or ΔR2-R4) DNA (147 bp) were described previously (31). The sequence of primer oriR2R4 is 5′-GAATGAGGGGTTATACACAACTC. DnaA and *tma*DnaA proteins were purified as described previously (50, 51).

Filter Retention Assay—This assay was performed as described previously (29, 50). DnaA was incubated on ice for 15 min in buffer N (25 μl) containing various concentrations of [α-^{32}P]ATP or [^{3}H]ADP, followed by filtration on nitrocellulose membranes. Retention was measured by liquid scintillation counting. When *tma*DnaA was used, *tma*DnaA (1.9 pmol) was incubated at 38 °C for 5 min in Buffer N′ (25 μl) containing various concentrations of [α-^{32}P]ATP. After the addition of 2.5 mM magnesium acetate, samples were incubated on ice for 15 min, followed by filter retention.

DUE Unwinding Assay—This assay was performed as described previously (31). Briefly, DnaA was incubated for 3 min at 38 °C in buffer P (20 μl) containing IHF (55 nM) and a supercoiled form of pBSoriC (4 nM), followed by incubation for 200 s at the same temperature in the presence of P1 nuclease (4 units; Yamasa Co.). These reactions were terminated by the addition of 0.5% SDS, and DNA was extracted with phenol/chloroform and precipitated with ethanol. Then a portion (one-tenth volume) was digested with AlwNI, followed by electrophoresis in a 1% agarose gel and ethidium bromide staining. When *tma*DnaA was used, reactions were performed at 48 °C using pOZ14 DNA and HU protein instead of pBSoriC and IHF, respectively.

Minichromosome Replication Assay—This assay was performed essentially as previously described (29). Briefly, a reaction mixture (25 μl) contained M13KEW101 *oriC* plasmid RF I (200 ng), ATP (or ADP)-DnaA, DnaB, DnaC, DnaG, HU, gyrase, single-stranded DNA-binding protein, DNA polymerase III holoenzyme, rNTPs, and dNTPs, including [α-^{32}P]dATP.

ssDUE Binding Analysis by Electrophoretic Mobility Shift Assay (EMSA)—This assay was performed as described previously (31). Briefly, ATP-DnaA and 2.5 nM ^{32}P-labeled ss-dsDUE (ssDUE-dsR1 or ssDUE-dsNon) were incubated for 10 min at 30 °C in buffer G (10 μl) containing 4 μg/ml poly(dA-dT)-(dA-dT) and 4 μg/ml poly(dI-dC)-(dI-dC) in the presence of DARΔR1 DNA (5 nM), followed by 4% PAGE at room temperature.

DNase I Footprint Assay—This assay was performed as previously described (24, 28, 29). Briefly, DnaA was incubated at 30 °C for 10 min in buffer F (10 μl) containing a 419-bp ^{32}P-end-labeled *oriC* fragment (5.5 ng, 2 nM) and 3 mM ATP or ADP, followed by a 4-min incubation at the same temperature in the presence of DNase I (0.63 milliunit). After the reaction was stopped by the addition of 0.5% SDS, DNA was extracted with phenol/chloroform, precipitated with ethanol, and analyzed by 5% sequencing gel electrophoresis.

Pull-down Assay Using oriC—This assay was performed essentially as described previously (31, 42). Biotinylated *oriC* DNA (10 nM) was incubated at 4 °C for 10 min in buffer G (10 μl) containing DnaA (0 or 0.5 μM), HisDnaB (0–0.5 μM), and DnaC (0–0.5 μM). Biotinylated DNA-bound materials were recovered using streptavidin-coated beads (Promega), washed in buffer G′ (12.5 μl), dissolved in SDS sample buffer, and analyzed by SDS-10% PAGE and silver staining. To deduce the amounts of bead-bound DNA, the biotinylated DNA remaining in the streptavidin-unbound fraction was extracted with phenol/chloroform, precipitated with glycogen in ethanol, and analyzed quantitatively by 4% PAGE and ethidium bromide staining. These values are used for subtraction to deduce the amounts of bead-bound DNA, as described previously (31).

Analysis of oriC Subcomplexes by EMSA—This assay was performed as described previously (24). The DF-LL or RL-RE DNA (350 fmol or 35 nM) was incubated at 30 °C for 10 min in buffer GS (10 μl) containing ATP-DnaA and λDNA (200 ng) as a competitor and analyzed at room temperature by 2% agarose gel electrophoresis (5.66 V/cm, 70 min), Gel-Star (TAKARA Co.) staining, and densitometric scanning.

Reconstituted RIDA Assay—The RIDA reactions were reconstituted *in vitro* and performed as described previously (12–14). Briefly, ATP-DnaA was incubated for 20 min at 30 °C in buffer R containing ADP-bound Hda-cHis (ADP-Hda) and plasmid DNA-loaded clamps that were isolated by gel filtration spin column chromatography.

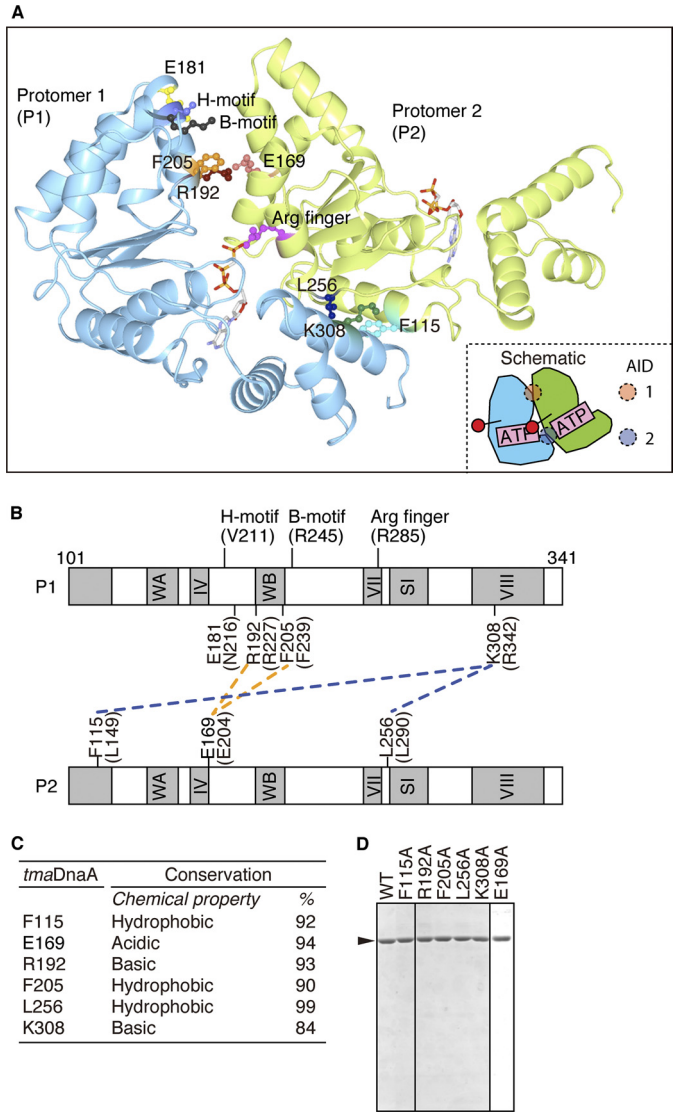

*tma*DnaA	Conservation	
	Chemical property	%
F115	Hydrophobic	92
E169	Acidic	94
R192	Basic	93
F205	Hydrophobic	90
L256	Hydrophobic	99
K308	Basic	84

FIGURE 2. **Homology modeling and purification of mutant *tma*DnaA proteins.** *A*, the monomeric *tma*DnaA AAA+ domain structures (Protein Data Bank entry 2Z4S) were superimposed onto an oligomeric structure of the *A. aeolicus* DnaA ortholog (Protein Data Bank entry 2HCB). Only two *tma*DnaA protomers are shown for simplicity using *ribbons* and a *schematic representation*. Each protomer is *colored* differently. The residues investigated in this study are represented by a *ball-and-stick model*. *B*, possible interactions (*dashed lines*) between two *tma*DnaA protomers are indicated using a linear map of the *tma*DnaA AAA$^+$ domain. Representative motifs of AAA$^+$ domain and the residues investigated in this study are indicated. Corresponding *E. coli* DnaA residues are indicated in *parentheses*. *WA*, Walker A; *IV*, box IV, *WB*, Walker B; *VII*, box VII; *SI*, sensor 1; *VIII*, box VIII. *C*, sequence homology analysis. Protein sequences of ~1000 DnaA orthologs were obtained from the Comprehensive Microbial Resource and aligned using the ClustalW program (available from the Max-Planck Institute for Developmental Biology Web site). The number of DnaA residues with the same chemical property (hydrophobic, acidic, or basic) at the position corresponding to the *tma*DnaA Phe-115, Glu-169, Arg-192, Phe-205, Leu-256, or Lys-308, respectively, was indicated as a percentage (*Conservation* (%)). *D*, mutant *tma*DnaA proteins were purified, and each protein (0.4 μg) in the final fraction was analyzed by SDS-12% PAGE and Coomassie Brilliant Blue staining.

RESULTS

Homology Modeling and Selection of Specific Residues—To identify specific DnaA residues required for inter-DnaA interactions during DUE unwinding, we used *tma*DnaA, the only protein that met both of our two requirements: 1) a protein whose AAA+ domain crystal structure has been determined and 2) a protein that forms open complexes *in vitro* using the cognate *oriC* (29, 50). We first constructed a homology model of the *tma*DnaA multimer using crystal structures of a monomeric ADP-*tma*DnaA AAA+ domain and a homotetrameric AMPPCP (a non-hydrolyzed ATP analog)-bound *Aquifex aeolicus* DnaA AAA+ domain (Fig. 2, *A* and *B*) (49). In this

TABLE 1

ATP binding activity of the mutant *tma*DnaA

WT and mutant *tma*DnaA proteins (1.9 pmol) were incubated at 0 °C for 15 min in the presence of various amounts (0–1 μM) of [α-^{32}P]ATP, followed by filtration on a nitrocellulose membrane. Dissociation constants (K_d) and the stoichiometries were determined using a Scatchard plot (16).

*tma*DnaA	K_d	Stoichiometry
	nM	
WT	25	0.68
F115A	20	0.64
E169A	18	0.61
R192A	14	0.86
F205A	22	0.91
L256A	21	0.44
K308A	22	0.83

model, several DnaA residues are exposed close to the adjacent protomer. Of these, we focused on *tma*DnaA Phe-115, Glu-169, Arg-192, Phe-205, Leu-256, and Lys-308 residues, due to the high conservation among eubacterial DnaA orthologs (Fig. 2*C*).

These residues are subdivided into two groups: ATP-DnaA-specific interactive locus for DUE unwinding (AID)-1 and -2. AID-1 contains *tma*DnaA Glu-169, Arg-192, and Phe-205 residues, which reside close to the B/H motifs (Fig. 2*A*). Notably, *tma*DnaA Glu-169 and Arg-192 can form an ionic bond (Fig. 2*B*). AID-2 contains *tma*DnaA Phe-115, Leu-256, and Lys-308 residues. *tma*DnaA Phe-115 and Leu-256 residues can form a hydrophobic interaction with the flanking α-helix, including the *tma*DnaA Lys-308 residue (Fig. 2*B*).

Mutant tmaDnaA Proteins Are Defective in DUE Unwinding Activity—To investigate whether mutations in these residues affect DUE unwinding activity, we first constructed plasmids that overexpress *tma*DnaA proteins carrying an alanine substitution. We then overexpressed and purified the mutant DnaA proteins using a method previously used to isolate WT *tma*DnaA (50). Like WT *tma*DnaA, these mutant proteins remained soluble during the preparation of cleared lysates and incubation at 60 °C. After gel filtration chromatography, the final step of purification, each of these mutant proteins eluted as a single peak at a position corresponding to its monomeric form, similar to the WT *tma*DnaA. The final fractions of mutant *tma*DnaA proteins were of >90% purity, as determined by SDS-PAGE (Fig. 2*D*). Moreover, a filter retention assay revealed that all of the mutant *tma*DnaA proteins retained affinity for ATP at a level similar to that of WT *tma*DnaA (Table 1).

Next, we performed a P1 nuclease assay to assess the DUE unwinding activity of the mutant *tma*DnaA proteins. In this assay, ATP-*tma*DnaA unwinds the DUE duplex of a supercoiled form of the *tma-oriC* plasmid, pOZ14, in a manner dependent on torsional stress and thermal energy (50). The resulting ssDNA is susceptible to cleavage by P1 nuclease. Following digestion with AlwNI, 2.1- and 1.0-kb fragments are produced (Fig. 3, *A–C*). The results of this experiment indicated that all of the mutant *tma*DnaA proteins are inactive in DUE unwinding activity (Fig. 3), which suggests that *tma*DnaA Phe-115, Glu-169, Arg-192, Phe-205, Leu-256, and Lys-308 are required for DUE unwinding, and is consistent with the idea that two distinct interfaces (*i.e.* AID-1 and -2 in Fig. 2*A*) between DnaA protomers are crucial for the formation of initial complexes.

Identification of E. coli DnaA Mutants Defective in Initiation in Vivo—To determine the importance of these residues *in vivo*, we constructed pKA234-derivative plasmids encoding *E. coli* DnaA mutant proteins that have Ala substitutions at the positions corresponding to the *tma*DnaA residues indicated above, and these plasmids were used for complementation tests (Table 2) (29). pKA234 is a pBR322-based multicopy vector bearing a WT *dnaA* gene that is located downstream of an arabinose-inducible promoter, but in these experiments, only leaky expression in the absence of arabinose was used for *dnaA* expression, as described previously (14, 24, 29).

First, we used a temperature-sensitive *dnaA46* mutant strain, KA413, as a host. The DnaA-producing plasmids bearing WT or mutant *dnaA* alleles were introduced into KA413 cells, and the transformants were incubated overnight at 30 or 42 °C (Table 2, experiment A). All of the plasmids bearing the mutant *dnaA* alleles, except for *dnaA F239A*, did not support colony formation at 42 °C, whereas they supported colony formation at 30 °C with an efficiency similar to the WT *dnaA* plasmid.

The plasmid bearing *dnaA F239A* supported colony formation of KA413 cells at 42 °C (Table 2, experiment A), raising the possibility that DnaA F239A may retain residual activity and may induce initiation when moderately overproduced. Alternatively, DnaA F239A may form functional hetero-oligomers with DnaA46 protein in KA413 cells, although DnaA F239A itself is inactive. Considering these possibilities, we next assessed the initiation activity of DnaA F239A by using a low copy mini-R derivative plasmid and a *dnaA*-disrupted strain, KA451 (*rnhA*::*cat dnaA*::Tn*10*), as a host (Table 2, experiment B). In KA451, the lack of the *rnhA* gene activates an alternative *oriC*-independent initiation system and allows *dnaA*-independent slow cell growth (52). Plasmid pOZ18 is a low copy mini-R derivative bearing WT *rnhA* and *dnaA* genes, each of which has its intact promoter (51). When KA451 and a WT strain, KH5402-1, were transformed with pOZ18, transformants were obtained at 30 °C after 20 h with the same efficiency (Table 2, experiment B), which was similar to our previous results (29). In KA451 cells bearing pOZ18, the plasmid-encoded *rnhA* gene represses the *oriC*-independent replication system, and the plasmid-encoded *dnaA* gene activates the *oriC* initiation system instead, which results in colony formation within 20 h. When a pOZ18 derivative (pmF239A) bearing *dnaA F239A* was used for transformation, the colony formation was sustained by KH5402-1 but not KA451 (Table 2, experiment B), which is similar to the results obtained with the control vector pRRNH bearing *rnhA* alone. These results indicate that DnaA F239A is basically inactive in initiation at *oriC in vivo* at 30 °C.

Taken together, these results reveal that the *E. coli* DnaA Leu-149, Glu-204, Arg-227, Phe-239, Leu-290, and Arg-342 residues are required for initiation at *oriC in vivo*, consistent with the idea that two distinct interfaces (*i.e.* AID-1 and -2 in Fig. 2*A*) between DnaA protomers are crucial for the formation of initial complexes.

E. coli DnaA R227A and L290A Are Inactive in DUE Unwinding and Replication Initiation—To further elucidate the role of these newly identified functional structures, we focused on representative mutant *dnaA* alleles (*dnaA R227A* for AID-1 and

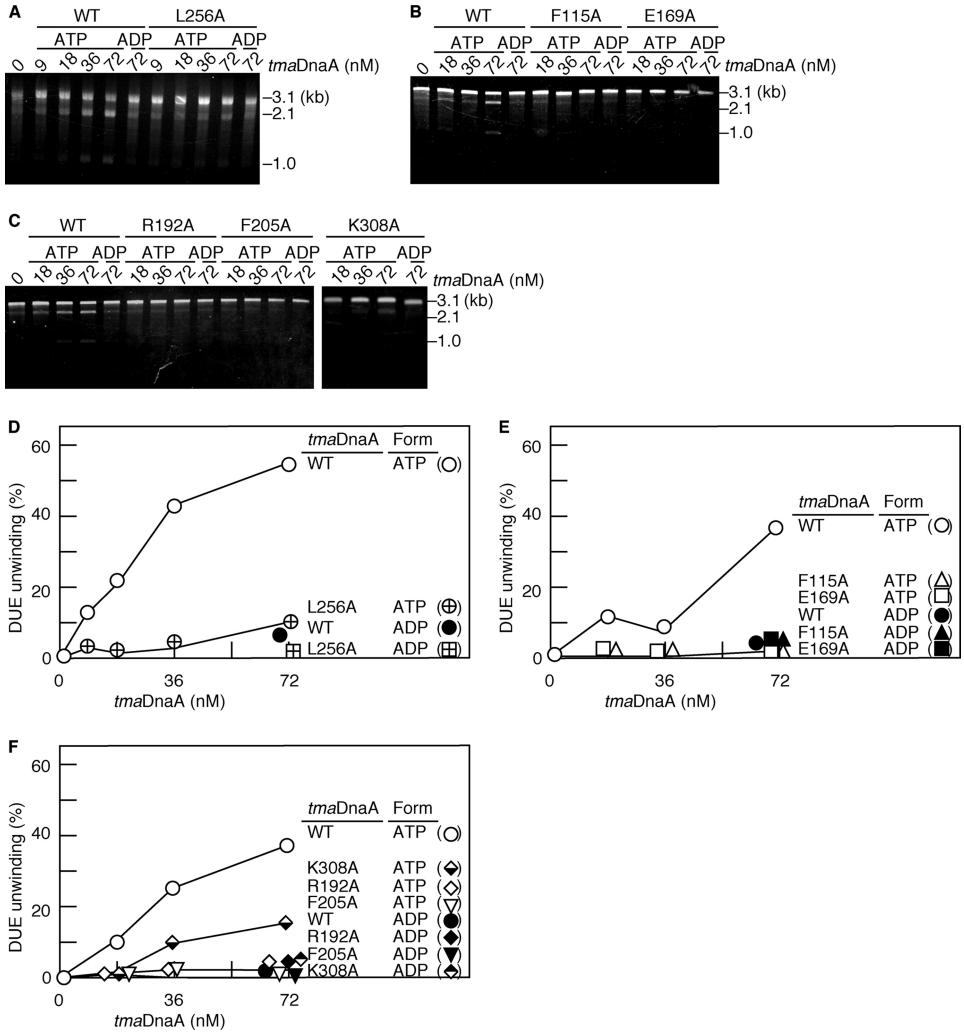

FIGURE 3. ***tma*DnaA mutants defective in open complex formation.** The WT or mutant *tma*DnaA protein (F115A, E169A, R192A, F205A, L256A, and K308A) (1.5 μM) was preincubated with 3 μM ATP or ADP. The resultant ATP form (*ATP*) or ADP form (*ADP*) of *tma*DnaA (0–300 nM) was incubated at 48 °C for 10 min in buffer containing the supercoiled form of the *tma-oriC* plasmid, pOZ14 (200 fmol or 4 nM), followed by digestion with P1 nuclease (10 units, 50 s at 48 °C). DNA products were purified and digested with AlwNI, followed by analysis using a 1% agarose gel and ethidium bromide staining. The gel images are shown (*A–C*). The number of P1 nuclease-digested *oriC* DNA molecules per molecule of input DNA is shown as a percentage (*DUE unwinding* (%)) (*D–F*).

TABLE 2

Plasmid complementation tests

For experiment A (Expt. A), KA413 (*dnaA46*) cells were transformed with a plasmid bearing the indicated *dnaA* allele and incubated on LB agar plates containing thymine (50 μg/ml) and ampicillin (50 μg/ml) at 30 °C for 21 h or at 42 °C for 12 h. Transformation efficiencies and the ratios are shown. For experiment B (Expt. B), KH5402–1 (WT *dnaA*) cells and KA451 (*dnaA*::Tn*10 rnhA*::*cat*) cells were transformed with mini-R derivative plasmids bearing WT *rnhA* and the indicated *dnaA* allele and incubated as above at 30 °C for 20 h. In both experiments, the corresponding *tma*DnaA residues are indicated in parentheses.

	Host	Plasmid	Allele	(*tma*DnaA)	Transformation efficiency		
					30 °C	42 °C	42 °C/30 °C
					cfu/μg DNA		
Expt. A	KA413	pKA234	*WT*		6.2×10^5	6.6×10^5	1.1
		pL149A	*L149A*	*(F115A)*	7.2×10^5	$<5.0 \times 10^2$	$<6.9 \times 10^{-4}$
		pE204A	*E204A*	*(E169A)*	9.9×10^5	$<1.0 \times 10^2$	$<1.0 \times 10^{-4}$
		pR227A	*R227A*	*(R192A)*	4.2×10^5	$<5.0 \times 10^2$	$<1.2 \times 10^{-3}$
		pF239A	*F239A*	*(F205A)*	4.3×10^5	4.2×10^5	1.0
		pL290A	*L290A*	*(L256A)*	6.9×10^5	$<5.0 \times 10^2$	$<7.2 \times 10^{-4}$
		pR342A	*R342A*	*(K308A)*	1.5×10^5	$<2.0 \times 10^3$	$<1.3 \times 10^{-3}$
		pING1 (vector)	*None*		6.6×10^5	$<2.0 \times 10^3$	$<3.0 \times 10^{-3}$
Expt. B	KH5402-1	pOZ18	*WT*		4.2×10^5		
		pmF239A	*F239A*	*(F205A)*	9.0×10^4		
		pRRNH (vector)	*None*		5.2×10^5		
	KA451	pOZ18	*WT*		6.6×10^3		
		pmF239A	*F239A*	*(F205A)*	<30		
		pRRNH (vector)	*None*		<30		

TABLE 3

ATP and ADP binding activity of the mutant *E. coli* DnaA

The kinetics were determined using the same method as described in the legend for Table 1.

DnaA	ATP		ADP	
	K_d	Stoichiometry	K_d	Stoichiometry
	nM		*nM*	
WT	35	0.28	53	0.24
R227A	73	0.41	64	0.35
L290A	90	0.25	49	0.14

dnaA L290A for AID-2). Arg-227 and Leu-290 are most highly conserved in protomer 1 and 2, respectively, of a modeled dimer (Fig. 2, *B* and *C*). DnaA R227A and L290A were purified according to a method used previously for WT DnaA purification (29). A filter retention assay revealed that these mutant DnaA proteins retained the ability to bind both ATP and ADP (Table 3).

The P1 nuclease assay demonstrated that these mutant DnaA proteins are inactive in DUE unwinding, which indicates that DnaA Arg-227 and Leu-290 are required for open complex formation (Fig. 4, *A* and *B*). In addition, those mutant DnaA proteins were inactive for *oriC* plasmid replication in an *in vitro* system reconstituted with purified proteins (Fig. 4*C*). This is consistent with the data showing that these residues are crucial for *in vivo* initiation (Table 2) and that the corresponding *tma*DnaA residues Arg-192 and Leu-256 are crucial for DUE unwinding (Fig. 2).

DnaA Asn-216 is located in close proximity to Arg-227 (Fig. 2). DnaA N216A is fully active in replication initiation (29) and in DUE unwinding (supplemental Fig. 1), consistent with the specific role for Arg-227.

DnaA R227A and L290A Are Inactive in ssDUE Binding—After DUE unwinding, the resultant upper strand (T-rich strand) ssDUE binds to ATP-DnaA multimers formed on the LL region, which stabilizes the unwound state of DUE and promotes initiation (29, 31) (Fig. 1). The B/H motifs of DnaA bind ssDUE directly (29, 40). The ATP-DnaA-DF subcomplex also stimulates recruitment of its flanking ssDUE to the ATP-DnaA-LL subcomplex in this reaction (31) (Fig. 1). To assess the ssDUE binding and ssDUE recruiting activity of these mutants, we performed EMSA using a 5′-tailed ss-dsDUE fragment containing ssDUE and dsDNA bearing the DnaA box R1 (ssDUE-dsR1) and a non-sense sequence (ssDUE-dsNon). As demonstrated previously using WT ATP-DnaA (31), ssDUE-dsR1 binds to ATP-DnaA multimers formed on R1-deleted DAR more efficiently than those formed on ssDUE-dsNon (Fig. 5). Unlike WT ATP-DnaA, ATP-DnaA R227A and L290A bound neither ssDUE-dsR1 nor ssDUE-dsNon (Fig. 5), which indicates that these mutant proteins are inactive in ssDUE binding and recruiting activity, although the Arg finger and B/H motifs are intact.

DnaA R227A and L290A Impair DnaA Subcomplex Formation on the LL Region but Not the RL-RE Region—To investigate the conformational change of ATP-DnaA-specific multimers formed on *oriC*, we performed DNase I footprint experiments (24, 28, 29). DnaA proteins were incubated with an *oriC* fragment at 30 °C in the presence of ATP or ADP, followed by DNase I. As shown previously, WT DnaA bound to DnaA-

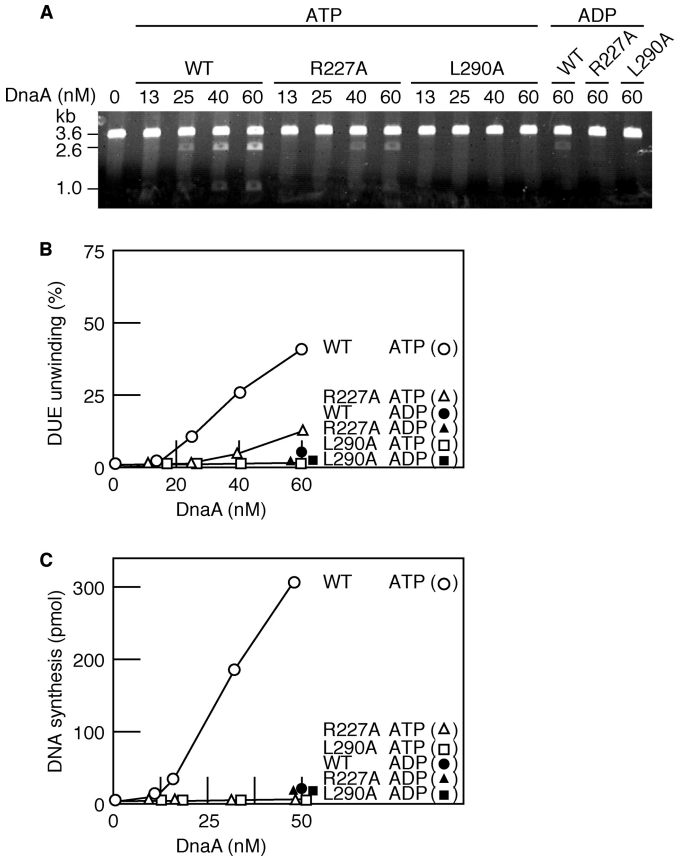

FIGURE 4. **Analysis of *E. coli* DnaA R227A and L290A in DUE unwinding and minichromosome replication.** *A* and *B*, DUE unwinding assay. The WT or mutant DnaA protein (R227A and L290A) (1.5 μM) was preincubated with 3 μM ATP or ADP. The resultant ATP form (*ATP*) or ADP form (*ADP*) of DnaA was incubated at 38 °C for 3 min in buffer containing the supercoiled form of pBS*oriC* and IHF, followed by digestion with P1 nuclease. The number of P1 nuclease-digested *oriC* DNA molecules per molecule of input DNA was analyzed by 1% agarose gel electrophoresis and ethidium bromide staining (*A*) and is shown as a percentage (*DUE unwinding* (%)) (*B*). *C*, minichromosome replication assay. The ATP form (*ATP*) or ADP form (*ADP*) of WT or mutant DnaA protein (R227A and L290A) was incubated at 30 °C for 10 min in buffer containing the supercoiled form of an *oriC* plasmid M13KEW101 and purified replication proteins (29).

binding sites R1 and R4 with high affinity, regardless of its nucleotide form (Fig. 6). Moreover, ATP-DnaA, but not ADP-DnaA, efficiently bound to ATP-DnaA-preferential binding sites (R2 and R3, M, I1–I3, τ1 and τ2, and C1–C3) (Fig. 6). Notably, the binding activity of ATP-DnaA R227A and L290A to ATP-DnaA-preferential binding sites (R5, I1 and I2, and τ1 and τ2) within the LL region was lower than that of WT ATP-DnaA (Figs. 6 and 7); the footprint patterns by the mutant proteins in this region were overall intermediate between those of WT ATP-DnaA and ADP-DnaA. Also, DnaA L290A was slightly less active in this binding than DnaA R227A (Figs. 6 and 7). In contrast, the mutant proteins retained full affinity for the ATP-DnaA-preferential binding sites (R2 and R3, I3, and C1–C3) within the RL-RE regions (Figs. 6 and 7); the footprint patterns within this region differed evidently compared with those of ADP-DnaA. The slight decrease in mutant DnaA binding observed in the RL-RE region might be an indirect consequence of unstable binding to the LL region and deceased cooperativity. The binding affinity of the mutant proteins to the R1 and R4 sites was similar to that of WT DnaA. These results

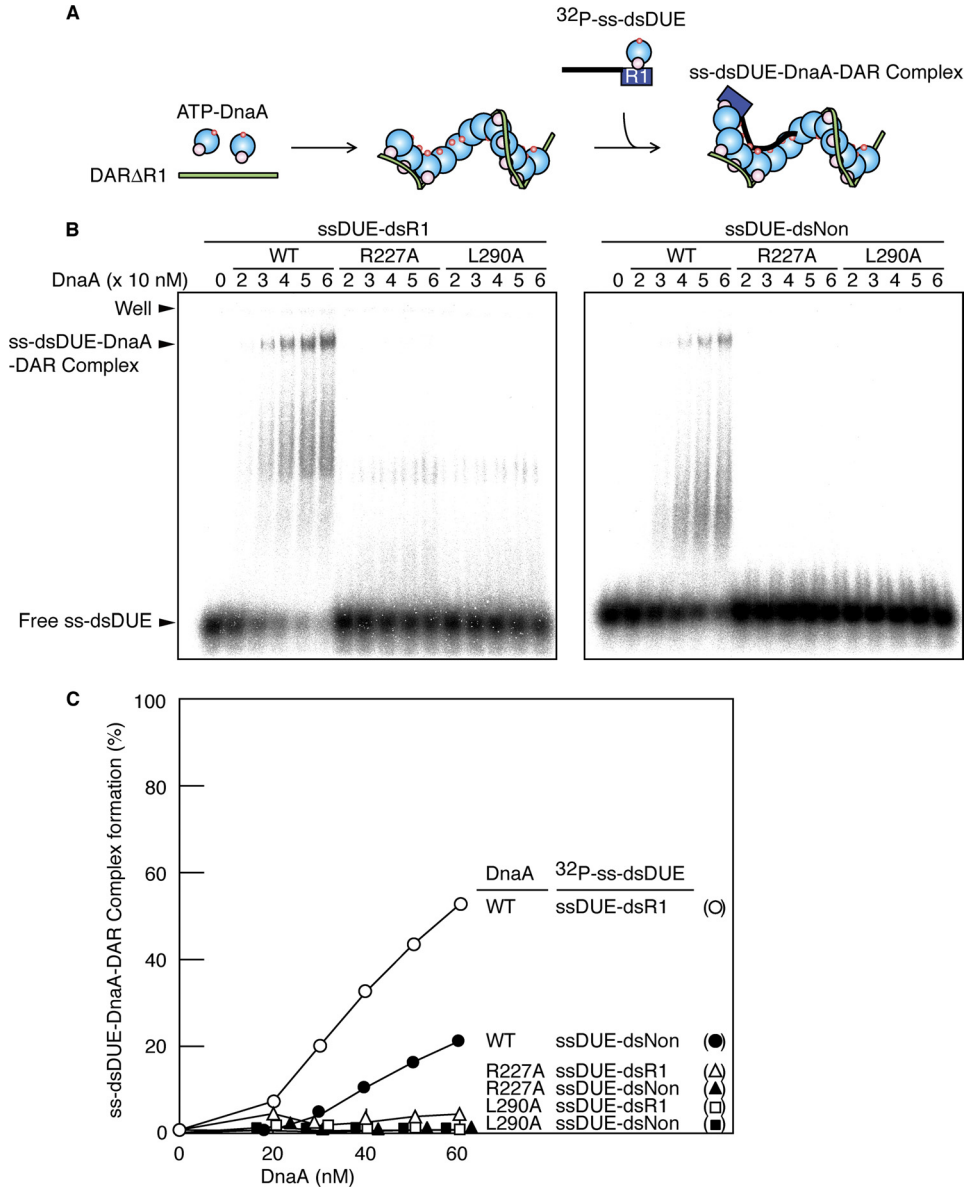

FIGURE 5. **ssDUE binding analysis of *E. coli* DnaA R227A and L290A.** *A*, schematic of the ssDUE binding assay. ATP-DnaA was incubated with DAR and end-labeled ss-dsDUE, followed by EMSA. For simplicity, only the DnaA domains III and IV are illustrated by *blue* and *pink balls*, respectively. The DnaA B/H motifs within domain III are indicated by *small red balls*. DARΔR1 (*green bar*) and ^{32}P-labeled ssDUE (*black line*) conjugated to dsDNA bearing DnaA-binding site R1 (*blue box*) (ssDUE-dsR1) are also indicated. *ss-dsDUE*, ssDUE-dsR1, ssDUE-dsNon, or both. *B* and *C*, WT ATP-DnaA, ATP-DnaA R227A, or ATP-DnaA L290A (0–60 nM) was incubated with 5 nM DARDR1 and a 2.5 nM concentration of either ^{32}P-labeled ssDUE-dsR1 or ssDUE-dsNon, followed by EMSA. *ss-dsDUE*, ssDUE-dsR1 or ssDUE-dsNon. ssDUE-dsNon is the same as ssDUE-dsR1, except that the R1 site is replaced with a sequence with no affinity for DnaA. Radioactivity of the resultant gel was visualized (*B*). The amount of ss-dsDUE-DnaA-DAR complexes was quantified, and the amount of the complexes relative to the input ss-dsDUE was plotted as ss-dsDUE-DnaA-DAR complex formation (%) (*C*). Certain amounts of the complex were unstable during electrophoresis, yielding smeared DNA bands with moderate retardation in mobility. *Well*, gel well; *Free ss-dsDUE*, protein-free ss-dsDUE.

indicate that DnaA Arg-227 and Leu-290 residues play a crucial role in the formation of a stable ATP-DnaA multimer on the LL region. Evidently, the specific nucleoprotein structure in this region requires these residues, in addition to the DnaA Arg finger Arg-285 (24).

Furthermore, we investigated using EMSA the role for Arg-227 and Leu-290 residues in DnaA multimer formation activity on the DF-LL and RL-RE regions. DNA fragments consisting of the DF-LL or RL-RE region were incubated with ATP-DnaA proteins at 30 °C, followed by agarose gel electrophoresis (Fig. 8). WT ATP-DnaA formed multimers on each fragment, and intermediate complexes were only faint. This suggests that ATP-DnaA molecules cooperatively bind to each fragment under these conditions, consistent with our previous EMSA data (24, 29). Difference in multimer formation efficiency between the DF-LL and RL-RE regions would be due to the structural feature that the DF-LL region carries only the low affinity sites in addition to the high affinity site R1, whereas the RL-RE region carries the moderate affinity site R2 in addition to the high affinity site R4 (Fig. 1*A*). Notably, ATP-DnaA R227A and L290A proteins formed multimers less efficiently than WT ATP-DnaA on the DF-LL region (Fig. 8, *A* and *B*). Reduction in the efficiency of DnaA L290A was severer than that of DnaA R227A. In contrast, these mutant proteins formed multimers on the

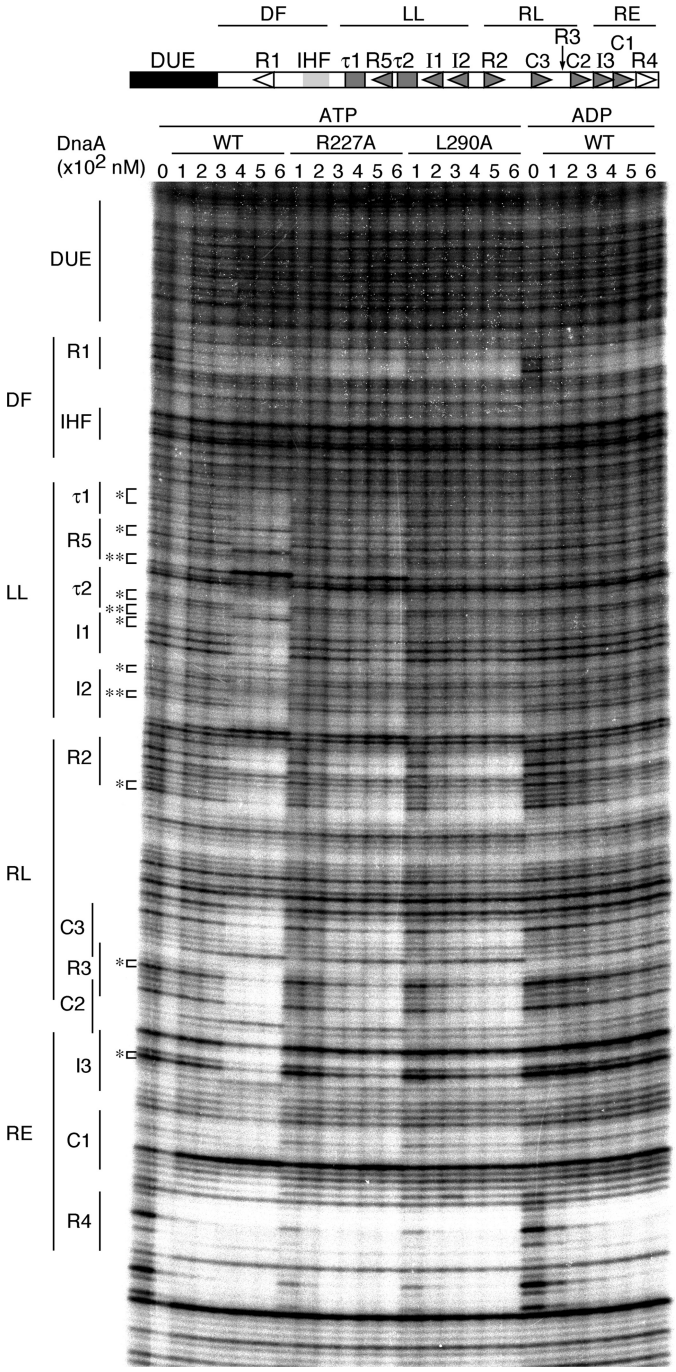

FIGURE 6. **DNase I footprint analysis.** Various concentrations (0–600 nM) of WT and mutant DnaA proteins were incubated for 10 min at 30 °C in buffer containing ^{32}P-labeled *oriC* DNA (419 bp) and 3 mM ATP or ADP, followed by digestion with DNase I. The resultant DNA fragments were analyzed on a 5% sequencing gel and visualized using a BAS2500 imager. The positions of the *oriC* subregions (DF, LL, RL, and RE), DnaA-binding sequences (R1–R5, I1–I3, τ1 and τ2, and C1–C3), and DUE are indicated. A schematic of the minimum *oriC* region is illustrated *above* the gel image. *Asterisks* indicate bands that are quantified in intensity for Fig. 7.

RL-RE region at a level comparable with WT DnaA (Fig. 8, *C* and *D*). These results coincide well with those in Figs. 6 and 7.

Taken together, these results suggest that the inter-DnaA interaction predicted in Fig. 2*A* is important for the DnaA-LL subcomplex, but not for the DnaA-RL-RE subcomplex, and that cooperative binding of the mutant DnaA proteins was reduced in the LL region. In addition, these data are consistent with the previous observation that the DnaA-LL subcomplex is required for ssDUE binding and *in vivo* initiation (31, 53) and our data showing that these residues are crucial for ssDUE binding *in vitro* and initiation *in vivo* (Fig. 5 and Table 2).

DnaA R227A and L290A Retain DnaB Binding Activity—Unlike DnaA monomers, DnaA multimers formed on DAR stably bind DnaB-DnaC complexes in a DUE unwinding-independent manner (31, 42) (Fig. 9*A*). DnaA domain I bears a specific site for DnaB binding (42, 43), but affinity of DnaA monomers for DnaB is weak (K_d of ~2 μM) (54), and these complexes cannot be isolated by a pull-down assay. However, when DnaA multimers are formed on DAR, DnaB binds to the multimers, and the resultant complexes can be stably isolated by a pull-down assay (31, 42). This is probably due to the fact that a single DnaA multimer has multiple DnaB binding sites, and DnaB is a stable homohexamer, thereby creating multiple binding sites and a linkage effect that drastically elevates the overall affinity between the two complexes (31, 42). In our previous study, when the right half of *oriC* was deleted, the recovery of DnaB molecules decreased by about one-half (31), which indicates the importance of DnaA multimer formation on both halves in DnaB binding. To test the DnaB binding activity of DnaA R227A and L290A in complex with DAR, we performed a similar pull-down assay. In this assay, ATP-DnaA, hexahistidine-fused DnaB (HisDnaB), and DnaC were co-incubated on ice in the presence of biotinylated *oriC* DNA. The resultant protein-DNA complexes were isolated using streptavidin beads (Fig. 9*A*).

Quantitatively consistent with previous results (31, 42), HisDnaB and DnaC were recovered with WT ATP-DnaA multimers bound to the *oriC* DNA (Fig. 9, *B* and *C*). The *oriC* complexes with ATP-DnaA R227A and L290A bound HisDnaB and DnaC at a level comparable with WT ATP-DnaA-*oriC* complexes (Fig. 9, *B* and *C*), which indicates that DnaA Arg-227 and Leu-290 are dispensable for the formation of DnaA multimers that are fully competent for binding the DnaB-DnaC complex.

Unlike DNase I footprint and EMSA (Figs. 7 and 8), this pull-down assay was performed on ice for stabilizing DnaA multimers. It should be noted that the number of ATP-DnaA molecules assembled onto *oriC* was indistinguishable between the WT and mutant DnaA proteins (Fig. 9, *B* and *C*). This coincides well with previous data showing that a considerable number of DnaA molecules form multimers on *oriC*, regardless of its nucleotide form (24, 28). Taken together, these results support the idea that DnaA Arg-227 and Leu-290 residues play a crucial role in the conformational change of the ATP-DnaA-LL subcomplex by enhancing inter-DnaA interaction on the LL region for ssDUE binding.

When open complexes are formed in the presence of DnaBC, DnaB is loaded on ssDUE and expands ssDNA regions (Fig. 9*A*). Unlike WT DnaA, DnaA R227A and L290A proteins, which were inactive in DUE unwinding (Fig. 4), were inactive in DnaB loading onto *oriC* DNA (supplemental Fig. 2).

DnaA R227A and L290A Proteins Are Fully Active in RIDA—In RIDA, ATP-DnaA interacts with Hda bound to DNA-loaded clamps. Detailed analysis of DnaA and Hda AAA+ structures in this interaction reveals that, at least in DnaA domain III, only

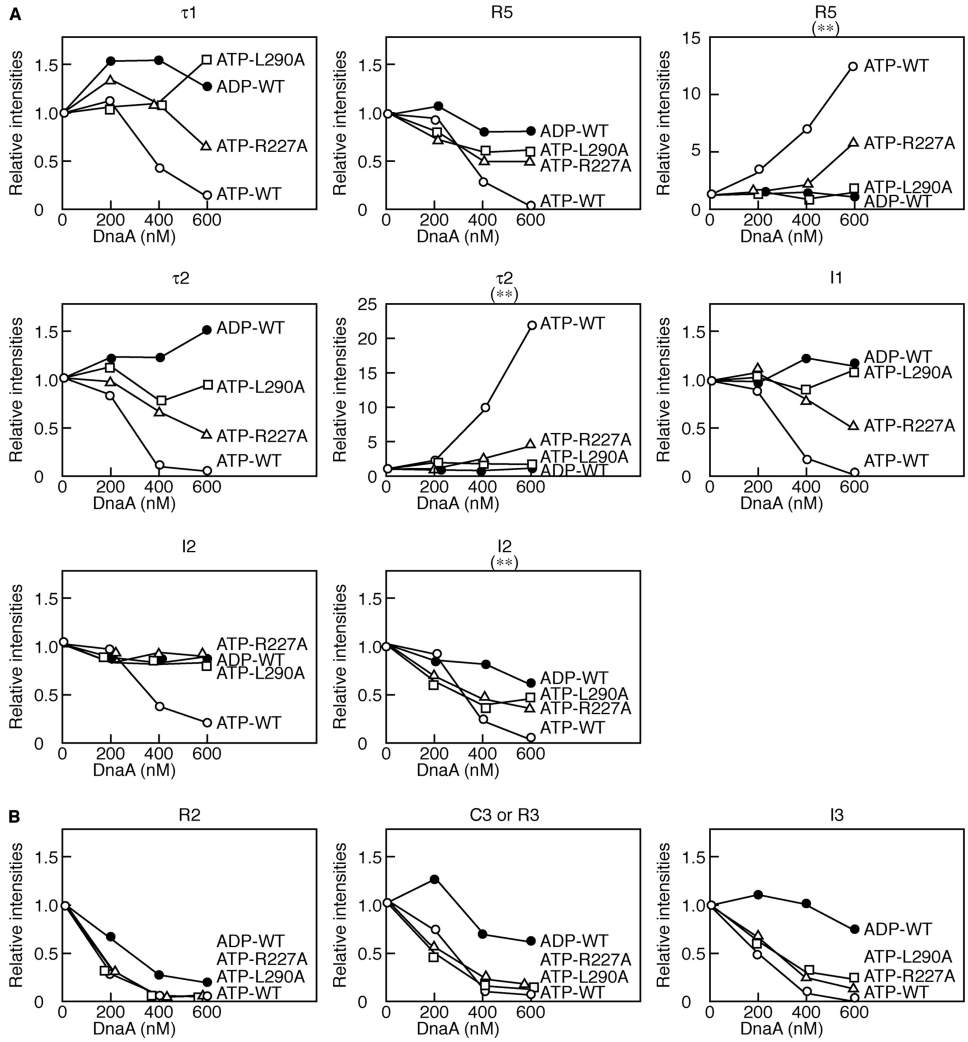

FIGURE 7. **Analysis of band intensities in DNase I footprint data.** The intensities of the representative bands indicated by *asterisks* in Fig. 6 were quantified in each *lane*. The intensities obtained in the absence of DnaA were referred to as 1.0, and the relative values at 200, 400, and 600 nM DnaA are presented. *A*, LL region. *B*, RL-RE region.

a region forming the ATP binding pocket is required for interaction with Hda (13) (see "Discussion"). In a RIDA-reconstituted system, the DnaA R227A and L290A proteins exhibit DnaA-ATP hydrolysis activity at a level similar to WT DnaA (Fig. 9*D*), further indicating that the main role of these residues is in promoting the inter-DnaA interaction required for *oriC* complex formation.

DISCUSSION

In this study, we revealed that specific *tma*DnaA residues within AID-1 and AID-2 are crucial for DUE unwinding. Moreover, *E. coli* DnaA mutants (R227A and L290A) that correspond to the representative *tma*DnaA AID mutants did not support initiation *in vivo*. Notably, we revealed that *E. coli* DnaA Arg-227 and Leu-290 play a specific role in DUE unwinding and ssDUE binding. Furthermore, our data demonstrate that, unlike WT ATP-DnaA, the ATP-DnaA R227A and L290A proteins do not support the formation of an ATP-DnaA-LL subcomplex that is active in ATP-DnaA-preferential site binding (Figs. 4–8). Defects in ssDUE binding and initiation activities of the mutant DnaA are reasonable in that the ATP-DnaA-LL subcomplex has the ability to bind ssDUE, which is a prerequisite for initiation (31). We thus propose that the residues we identified here are critical for the novel functional substructures of DnaA required for formation of the DnaA subcomplex that is competent for ssDUE binding. Taken together with the fact that AID-1 and -2 motifs are highly conserved among eubacterial DnaA orthologs, our findings suggest a common mechanism for eubacterial initial complexes.

Based on a homology model of *tma*DnaA multimers, AID-1 and -2 reside on distinct interfaces of the two protomers. We thus propose a novel mechanism in which these interfaces facilitate inter-ATP-DnaA interactions by promoting a unique conformational change in the ATP-DnaA-LL subcomplex that enhances the cooperative binding of DnaA protomers and ssDUE binding (Fig. 10). The residues identified were not required for the subcomplexes to bind to the ATP-DnaA-preferential sites within RL-RE regions or for the overall formation of DnaA multimers on DAR. These results indicate that DnaA multimers formed on DAR adopt distinct structures that correlate with their unique functions. This feature is consistent

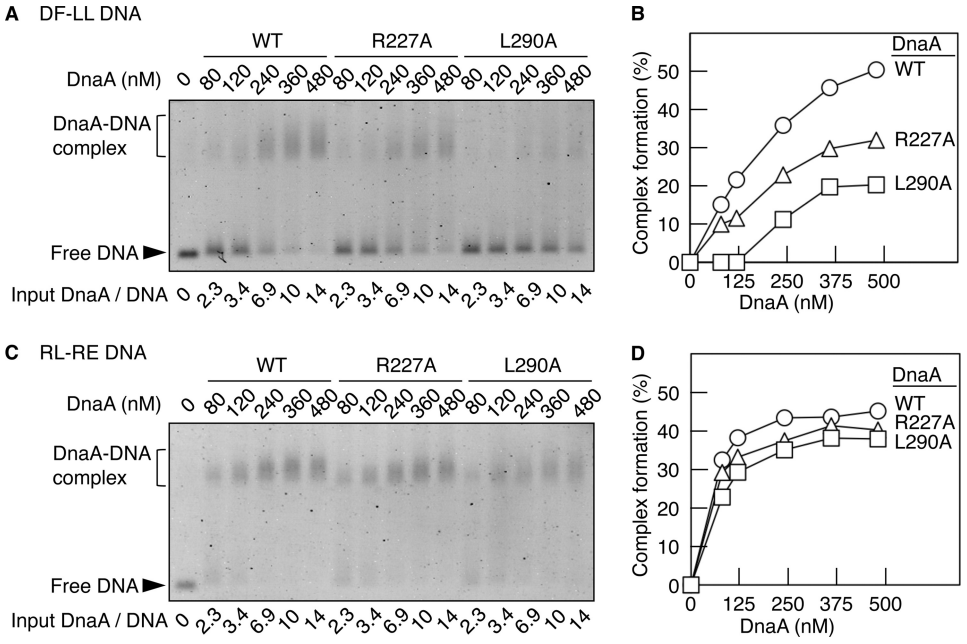

FIGURE 8. **Analysis of the DnaA complexes formed on the DF-LL and RL-RE regions.** The DF-LL DNA (*A* and *B*) or the RL-RE DNA (*C* and *D*) (350 fmol or 35 nM) were incubated at 30 °C for 10 min in buffer (10 μl) containing the indicated amounts of WT or mutant ATP-DnaA and analyzed by 2% agarose gel electrophoresis and Gel-Star staining. Representative gel images are shown in a *black and white* inverted mode (*A* and *C*). The molar ratio of input DnaA/DNA fragment is indicated *below* each *lane*. Each *lane* was analyzed by densitometric scanning, and proportions of DNA complexed with DnaA multimers (DnaA-DNA complex) to the total DNA were quantified and shown as a percentage (*Complex formation* (%)) (*B* and *D*). *Free DNA*, protein-free DNA.

with our model of the initial complex that achieves ssDUE recruitment (4, 15, 29, 31, 42) (Figs. 1 and 10) rather than the model of a continuous DnaA filament that assumes an overall uniform DnaA multimer on DAR and does not require different structural determinants in the LL region for DnaA-ssDUE binding (38–40).

Our data reveal that the role of *E. coli* DnaA Arg-227 and Leu-290 residues is distinct from that of the DnaA Arg-285 Arg finger as the key residue for the formation of ATP-DnaA-specific multimers on *oriC* (24). DnaA Arg-285 is required for initiation *in vivo* and *in vitro*. Structural analyses suggest that the side chain of the Arg finger is exposed on the protomer surface and recognizes ATP that is bound to the adjacent protomer, which can induce a conformational change in the overall DnaA multimer structure in the initial complexes (24, 29, 49). ATP-DnaA R285A is specifically inactive in binding to ATP-DnaA-preferential moderate and low affinity sites on the whole DAR and therefore forms inactive DnaA subcomplexes with the DAR-RL and RE regions as well as the LL region, like WT ADP-DnaA (24). Therefore, DnaA Arg-227 and Leu-290 are unique in that they are specifically required for the ATP-DnaA-LL subcomplex but not for the ATP-DnaA-RL-RE subcomplexes (Figs. 6–8). We propose that the open complexes are activated by at least two distinct mechanisms: 1) Arg finger-mediated conformational change of the overall ATP-DnaA-*oriC* structures and 2) local conformational change specific for ATP-DnaA-LL subcomplex (Fig. 10). In this context, we infer that the AID motifs, including *E. coli* DnaA Arg-227 and Leu-290, play a crucial role in the ATP-DnaA-LL subcomplex-specific conformational change.

It is conceivable that AID motif-mediated inter-DnaA interactions facilitate the projection of B/H motifs into the pore surface in the spiral-like DnaA multimers, creating an ssDUE-binding platform within the DnaA pore (Fig. 10). In the absence of the DnaA Arg-227 and Leu-290 residues, B/H motifs might not be projected fully in the pore and would result in the failure of ssDUE binding and open complex formation (Figs. 4 and 5). These ideas are consistent with the fact that the B/H motifs of only a subset of the DnaA protomers are required for an open complex (29).

In *E. coli*, DnaA assembly on *oriC* is also regulated in a manner coupled to the cell cycle (55–57). Whereas the DnaA-binding sites R1 and R4 are occupied by DnaA throughout the cell cycle (55–57), DnaA assembly on the LL and RL regions primarily occurs around the time of initiation (56). This is most likely due to the cell cycle-coordinated increase in intracellular ATP-DnaA levels (58), allowing the formation of ssDUE binding-competent ATP-DnaA subcomplexes (*i.e.* ATP-DnaA-LL subcomplex) (31). Formation efficiency or stability of ATP-DnaA-DF-LL subcomplex is lower than that of ATP-DnaA-RL-RE subcomplex (Fig. 8). Therefore, the formation of the ATP-DnaA-LL subcomplex may be an important rate-limiting reaction for open complex formation *in vivo* (31). In this context, we infer that AID motifs play a crucial role in the timely activation of initial complexes by regulating ATP-DnaA-LL subcomplex formation. In addition, as indicated *in vitro* by this study and a previous study by our group (42) (Fig. 9), DnaB binding to DnaA in complex with *oriC* can be achieved prior to DUE unwinding *in vivo*. This also supports a possible mechanism in which DUE unwinding facilitated by AID motifs, but not the DnaB-DnaA interaction, is a crucial rate-limiting step for regulating DnaB loading onto the unwound DUE of *oriC*.

Here, we showed that DnaA Arg-227 and Leu-290 residues are dispensable for the interaction with Hda in the RIDA reac-

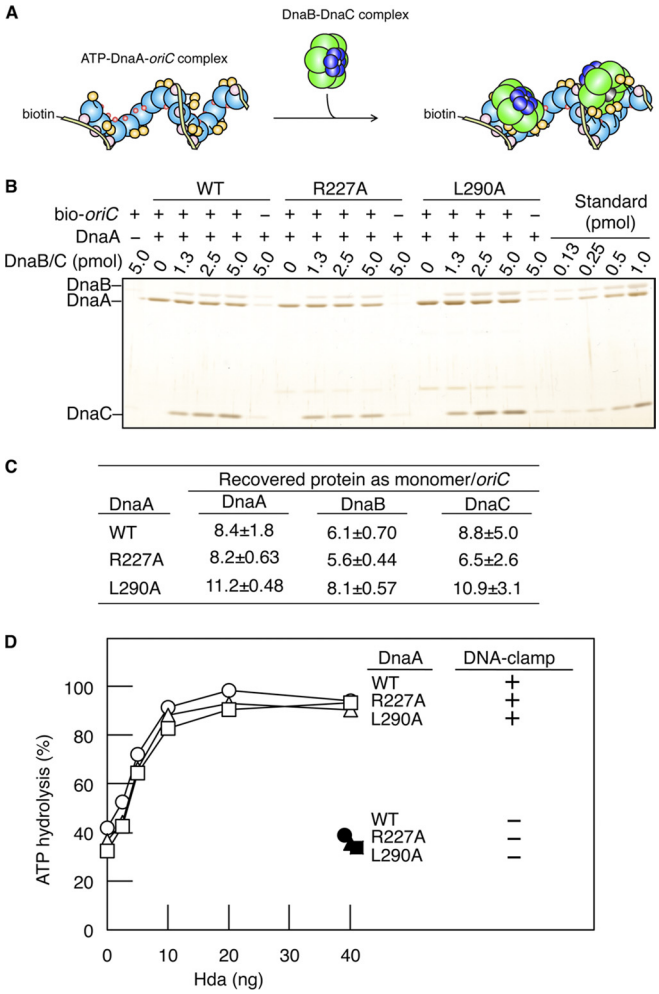

FIGURE 9. **Activity in DnaB binding and RIDA.** *A–C*, the *oriC* pull-down assay. A schematic of the assay is shown using the same *symbols* as in Fig. 1 in addition to symbols for the DnaB (*green*)-DnaC (*dark blue*) complex (*A*). WT ATP-DnaA, ATP-DnaA R227A, or ATP-DnaA L290A (5 pmol or 500 nM) and the bio-*oriC* DNA (419 bp, 100 fmol or 10 nM) were incubated on ice for 10 min in buffer (10 μl) containing various amounts (0, 1.3, 2.5, and 5 pmol) of His-DnaB-DnaC protein mixtures, followed by the pull-down assay, using streptavidin-coated magnetic beads. The bio-*oriC*-bound materials were analyzed by SDS-10% PAGE and silver staining (*B*). The recovered amounts of DnaA, HisDnaB, and DnaC in *A* were determined using standard curves of purified proteins. The recovered amounts of bio-*oriC* were deduced as described under "Experimental Procedures." These values were used to deduce the number of each protein recovered per bio-*oriC* (*C*). *D*, RIDA activity. WT DnaA (*circle*), DnaA R227A (*R227A*; *triangle*), or DnaA L290A (*L290A*; *square*) (500 nM) was preincubated on ice for 15 min with [α-^{32}P]ATP (0.8 μM), and portions of ATP-bound protein (0.5 pmol or 20 nM, final) were incubated at 30 °C for 20 min in buffer containing the indicated amounts of ADP-Hda and ADP (30 μM) in the presence (*open symbols*) or absence (*closed symbols*) of the DNA-loaded clamps (50 fmol or 2 nM as the clamp), followed by filter retention and thin layer chromatography. The ratio of ADP-DnaA to total ATP-/ADP-DnaA is shown as a percentage (*ATP hydrolysis*).

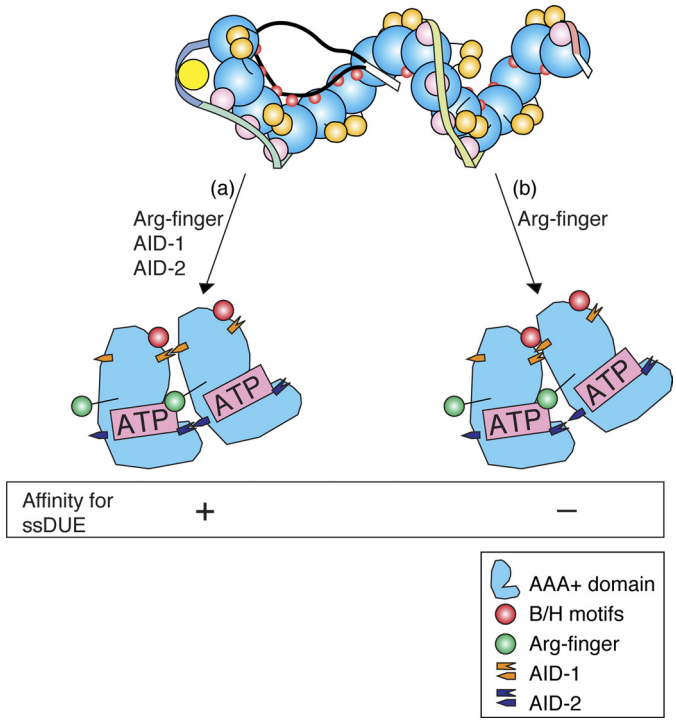

FIGURE 10. **Model for open complex architecture activated for ssDUE binding.** A model for an open complex including four distinct ATP-DnaA-DAR subcomplexes is illustrated using the same *symbols* as in Fig. 1*A*. Unlike other ATP-DnaA-DAR subcomplexes (*b*), the conformation of the ATP-DnaA-LL subcomplex is activated by inter-ATP-DnaA interactions mediated by the AID-1 and -2 motifs (*a*), which exposes the B/H motifs of the ATP-DnaA-LL subcomplex onto the pore surface, thereby increasing affinity for ssDUE. Plausible modes of inter-ATP-DnaA interactions are illustrated schematically using only the DnaA AAA+ domain for simplicity. See "Discussion" for details.

tion (Fig. 9*D*). Although Hda belongs to the AAA+ family and shares a significant level of sequence similarity with the DnaA AAA+ domain, little conservation is observed at the position corresponding to the DnaA AID motifs (*e.g.* DnaA Leu-290 corresponds to Gln-158) (18), which implies that different inter-AAA+ domain interaction modes exist for the open complex and the RIDA complex. This is also supported by previous data showing that the DnaA AAA+ sensor II motif Arg-334, a residue within the nucleotide-binding pocket, is required for DnaA-ATP hydrolysis but not open complex formation (13, 59). In agreement with this, mutant Hda analyses indicated that only the unique Hda residues that probably interact with the nucleotide-binding pocket-proximal substructure of DnaA are crucial for the interaction with DnaA (13). Unlike the RIDA reaction, open complex formation is a non-catalytic reaction, which would require a stable interaction via multiple interacting sites on the inter-AAA+ domain surface. In this context, we infer that DnaA AID motifs have evolved to play a specialized role in open complex formation but not in the RIDA reaction.

Like DnaA, typical AAA+ proteins adopt a ring- or spiral-like oligomer with the central pore (60). In well characterized AAA+ proteases, such as FtsH, HslU, and ClpX, these ATPases assemble into a hexameric ring with a central pore (60–62). These pore regions are required not only for substrate binding but also for translocation of the substrate in a manner coupled to the local conformational change of the pore, thereby triggering substrate proteolysis (63, 64). Therefore, pore formation and its conformational change play a common and crucial role in activating AAA+ protein complexes. In this context, it is reasonable that the AID motifs of DnaA play a specific role in the conformational change of the DnaA subcomplex on the LL region, as mentioned above.

In the case of the AAA+ proteases, alteration of pore conformation is coupled with the state of nucleotide binding of the protomer (*i.e.* ATP, ADP, or apo-form), which indicates that cycles of ATP binding and hydrolysis are important for induc-

ing local conformational changes of the pore in these complexes (61, 65). It should be noted that, unlike cycling, tight binding of ATP to DnaA is required for initiation (51, 59). This implies that DnaA protein structure is differentiated to utilize the specialized inter-ATP-DnaA interaction on the LL region, but not the DnaA-ATP hydrolysis, for achieving the local conformational change of the DnaA pore. These ideas are also consistent with the fact that DnaA is an unusual AAA+ protein that is stable as monomers in solution and is stimulated to form oligomers in a cooperative DNA binding-dependent manner (24, 25, 27, 66). ATP-DnaA multimers are also formed on the *dnaA* promoter region and repress transcription more efficiently than ADP-DnaA multimers (20). Distinct inter-DnaA interactions between *oriC* and the *dnaA* promoter region are proposed based on a finding that DnaA L366K sustains the ability to form functional multimers with the *dnaA* promoter region but not with *oriC* (48). This is basically consistent with our present finding that DnaA forms distinct multimers on the left and right halves of *oriC*. Based on structural and functional analysis, we propose a direct role for AID motifs in specific inter-DnaA interactions, while the question of whether Leu-366, located on a helix connecting domain III and IV, plays a direct role in inter-DnaA interactions remains to be explored.

Even in eukaryotes, replication initiation requires regulated duplex unwinding achieved by highly organized protein complexes (67, 68). These complexes include various AAA+ proteins, including ORC, Cdc6, and MCM (69). Moreover, electron microscopy analysis suggests that *Drosophila* ORC may form a DnaA-like spiral (70). Therefore, eukaryotic initial complexes may contain the AAA+ pore, which may induce conformational change during initiation by using mechanisms similar to the interprotein interactions mediated by the DnaA AID motifs.

Acknowledgments—We thank the Research Support Center, Graduate School of Medical Sciences, Kyushu University for DNA sequencing and Chika Odate for technical assistance.

REFERENCES

1. Bramhill, D., and Kornberg, A. (1988) Duplex opening by dnaA protein at novel sequences in initiation of replication at the origin of the *E. coli* chromosome. *Cell* **52,** 743–755
2. Messer, W. (2002) The bacterial replication initiator DnaA. DnaA and oriC, the bacterial mode to initiate DNA replication. *FEMS Microbiol. Rev.* **26,** 355–374
3. Duderstadt, K. E., and Berger, J. M. (2008) AAA+ ATPases in the initiation of DNA replication. *Crit. Rev. Biochem. Mol. Biol.* **43,** 163–187
4. Ozaki, S., and Katayama, T. (2009) DnaA structure, function, and dynamics in the initiation at the chromosomal origin. *Plasmid* **62,** 71–82
5. Leonard, A. C., and Grimwade, J. E. (2010) Regulating DnaA complex assembly. It is time to fill the gaps. *Curr. Opin. Microbiol.* **13,** 766–772
6. Kaguni, J. M. (2011) Replication initiation at the *Escherichia coli* chromosomal origin. *Curr. Opin. Chem. Biol.* **15,** 606–613
7. Makowska-Grzyska, M., and Kaguni, J. M. (2010) Primase directs the release of DnaC from DnaB. *Mol. Cell* **37,** 90–101
8. Soultanas, P. (2012) Loading mechanisms of ring helicases at replication origins. *Mol. Microbiol.* **84,** 6–16
9. Indiani, C., and O'Donnell, M. (2006) The replication clamp-loading machine at work in the three domains of life. *Nat. Rev. Mol. Cell Biol.* **7,** 751–761
10. Heller, R. C., and Marians, K. J. (2006) Replisome assembly and the direct restart of stalled replication forks. *Nat. Rev. Mol. Cell Biol.* **7,** 932–943
11. Katayama, T., Kubota, T., Kurokawa, K., Crooke, E., and Sekimizu, K. (1998) The initiator function of DnaA protein is negatively regulated by the sliding clamp of the *E. coli* chromosomal replicase. *Cell* **94,** 61–71
12. Su'etsugu, M., Nakamura, K., Keyamura, K., Kudo, Y., and Katayama, T. (2008) Hda monomerization by ADP binding promotes replicase clamp-mediated DnaA-ATP hydrolysis. *J. Biol. Chem.* **283,** 36118–36131
13. Nakamura, K., and Katayama, T. (2010) Novel essential residues of Hda for interaction with DnaA in the regulatory inactivation of DnaA. Unique roles for Hda AAA Box VI and VII motifs. *Mol. Microbiol.* **76,** 302–317
14. Keyamura, K., and Katayama, T. (2011) DnaA protein DNA-binding domain binds to Hda protein to promote inter-AAA+ domain interaction involved in regulatory inactivation of DnaA. *J. Biol. Chem.* **286,** 29336–29346
15. Katayama, T., Ozaki, S., Keyamura, K., and Fujimitsu, K. (2010) Regulation of the replication cycle. Conserved and diverse regulatory systems for DnaA and oriC. *Nat. Rev. Microbiol.* **8,** 163–170
16. Sekimizu, K., Bramhill, D., and Kornberg, A. (1987) ATP activates dnaA protein in initiating replication of plasmids bearing the origin of the *E. coli* chromosome. *Cell* **50,** 259–265
17. Fujimitsu, K., Su'etsugu, M., Yamaguchi, Y., Mazda, K., Fu, N., Kawakami, H., and Katayama, T. (2008) Modes of overinitiation, dnaA gene expression, and inhibition of cell division in a novel cold-sensitive hda mutant of *Escherichia coli*. *J. Bacteriol.* **190,** 5368–5381
18. Kato, J., and Katayama, T. (2001) Hda, a novel DnaA-related protein, regulates the replication cycle in *Escherichia coli*. *EMBO J.* **20,** 4253–4262
19. Camara, J. E., Breier, A. M., Brendler, T., Austin, S., Cozzarelli, N. R., and Crooke, E. (2005) Hda inactivation of DnaA is the predominant mechanism preventing hyperinitiation of *Escherichia coli* DNA replication. *EMBO Rep.* **6,** 736–741
20. Gon, S., Camara, J. E., Klungsøyr, H. K., Crooke, E., Skarstad, K., and Beckwith, J. (2006) A novel regulatory mechanism couples deoxyribonucleotide synthesis and DNA replication in *Escherichia coli*. *EMBO J.* **25,** 1137–1147
21. Riber, L., Fujimitsu, K., Katayama, T., and Løbner-Olesen, A. (2009) Loss of Hda activity stimulates replication initiation from I-box but not R4 mutant origins in *Escherichia coli*. *Mol. Microbiol.* **71,** 107–122
22. Charbon, G., Riber, L., Cohen, M., Skovgaard, O., Fujimitsu, K., Katayama, T., and Løbner-Olesen, A. (2011) Suppressors of DnaA(ATP) imposed overinitiation in *Escherichia coli*. *Mol. Microbiol.* **79,** 914–928
23. Fujimitsu, K., Senriuchi, T., and Katayama, T. (2009) Specific genomic sequences of *E. coli* promote replicational initiation by directly reactivating ADP-DnaA. *Genes Dev.* **23,** 1221–1233
24. Kawakami, H., Keyamura, K., and Katayama, T. (2005) Formation of an ATP-DnaA-specific initiation complex requires DnaA arginine 285, a conserved motif in the AAA+ protein family. *J. Biol. Chem.* **280,** 27420–27430
25. McGarry, K. C., Ryan, V. T., Grimwade, J. E., and Leonard, A. C. (2004) Two discriminatory binding sites in the *Escherichia coli* replication origin are required for DNA strand opening by initiator DnaA-ATP. *Proc. Natl. Acad. Sci. U.S.A.* **101,** 2811–2816
26. Rozgaja, T. A., Grimwade, J. E., Iqbal, M., Czerwonka, C., Vora, M., and Leonard, A. C. (2011) Two oppositely oriented arrays of low affinity recognition sites in oriC guide progressive binding of DnaA during *Escherichia coli* pre-RC assembly. *Mol. Microbiol.* **82,** 475–488
27. Schaper, S., and Messer, W. (1995) Interaction of the initiator protein DnaA of *Escherichia coli* with its DNA target. *J. Biol. Chem.* **270,** 17622–17626
28. Keyamura, K., Fujikawa, N., Ishida, T., Ozaki, S., Su'etsugu, M., Fujimitsu, K., Kagawa, W., Yokoyama, S., Kurumizaka, H., and Katayama, T. (2007) The interaction of DiaA and DnaA regulates the replication cycle in E. coli by directly promoting ATP DnaA-specific initiation complexes. *Genes Dev.* **21,** 2083–2099
29. Ozaki, S., Kawakami, H., Nakamura, K., Fujikawa, N., Kagawa, W., Park, S. Y., Yokoyama, S., Kurumizaka, H., and Katayama, T. (2008) A common mechanism for the ATP-DnaA-dependent formation of open complexes at the replication origin. *J. Biol. Chem.* **283,** 8351–8362

30. Yung, B. Y., Crooke, E., and Kornberg, A. (1990) Fate of the DnaA initiator protein in replication at the origin of the *Escherichia coli* chromosome *in vitro*. *J. Biol. Chem.* **265,** 1282–1285
31. Ozaki, S., and Katayama, T. (2012) Highly organized DnaA-oriC complexes recruit the single-stranded DNA for replication initiation. *Nucleic Acids Res.* **40,** 1648–1665
32. Weigel, C., and Seitz, H. (2002) Strand-specific loading of DnaB helicase by DnaA to a substrate mimicking unwound oriC. *Mol. Microbiol.* **46,** 1149–1156
33. Dillon, S. C., and Dorman, C. J. (2010) Bacterial nucleoid-associated proteins, nucleoid structure and gene expression. *Nat. Rev. Microbiol.* **8,** 185–195
34. Hwang, D. S., and Kornberg, A. (1992) Opening of the replication origin of *Escherichia coli* by DnaA protein with protein HU or IHF. *J. Biol. Chem.* **267,** 23083–23086
35. Ryan, V. T., Grimwade, J. E., Nievera, C. J., and Leonard, A. C. (2002) IHF and HU stimulate assembly of prereplication complexes at *Escherichia coli* oriC by two different mechanisms. *Mol. Microbiol.* **46,** 113–124
36. Weigel, C., Messer, W., Preiss, S., Welzeck, M., Morigen, and Boye, E. (2001) The sequence requirements for a functional *Escherichia coli* replication origin are different for the chromosome and a minichromosome. *Mol. Microbiol.* **40,** 498–507
37. Leonard, A. C., and Grimwade, J. E. (2005) Building a bacterial orisome. Emergence of new regulatory features for replication origin unwinding. *Mol. Microbiol.* **55,** 978–985
38. Speck, C., and Messer, W. (2001) Mechanism of origin unwinding. Sequential binding of DnaA to double- and single-stranded DNA. *EMBO J.* **20,** 1469–1476
39. Duderstadt, K. E., Mott, M. L., Crisona, N. J., Chuang, K., Yang, H., and Berger, J. M. (2010) Origin remodeling and opening in bacteria rely on distinct assembly states of the DnaA initiator. *J. Biol. Chem.* **285,** 28229–28239
40. Duderstadt, K. E., Chuang, K., and Berger, J. M. (2011) DNA stretching by bacterial initiators promotes replication origin opening. *Nature* **478,** 209–213
41. Felczak, M. M., Simmons, L. A., and Kaguni, J. M. (2005) An essential tryptophan of *Escherichia coli* DnaA protein functions in oligomerization at the *E. coli* replication origin. *J. Biol. Chem.* **280,** 24627–24633
42. Keyamura, K., Abe, Y., Higashi, M., Ueda, T., and Katayama, T. (2009) DiaA dynamics are coupled with changes in initial origin complexes leading to helicase loading. *J. Biol. Chem.* **284,** 25038–25050
43. Abe, Y., Jo, T., Matsuda, Y., Matsunaga, C., Katayama, T., and Ueda, T. (2007) Structure and function of DnaA N-terminal domains. Specific sites and mechanisms in inter-DnaA interaction and in DnaB helicase loading on oriC. *J. Biol. Chem.* **282,** 17816–17827
44. Nozaki, S., and Ogawa, T. (2008) Determination of the minimum domain II size of *Escherichia coli* DnaA protein essential for cell viability. *Microbiology* **154,** 3379–3384
45. Neuwald, A. F., Aravind, L., Spouge, J. L., and Koonin, E. V. (1999) AAA+. A class of chaperone-like ATPases associated with the assembly, operation, and disassembly of protein complexes. *Genome Res.* **9,** 27–43
46. Erzberger, J. P., Pirruccello, M. M., and Berger, J. M. (2002) The structure of bacterial DnaA. Implications for general mechanisms underlying DNA replication initiation. *EMBO J.* **21,** 4763–4773
47. Fujikawa, N., Kurumizaka, H., Nureki, O., Terada, T., Shirouzu, M., Katayama, T., and Yokoyama, S. (2003) Structural basis of replication origin recognition by the DnaA protein. *Nucleic Acids Res.* **31,** 2077–2086
48. Saxena, R., Rozgaja, T., Grimwade, J., and Crooke, E. (2011) Remodeling of nucleoprotein complexes is independent of the nucleotide state of a mutant AAA+ protein. *J. Biol. Chem.* **286,** 33770–33777
49. Erzberger, J. P., Mott, M. L., and Berger, J. M. (2006) Structural basis for ATP-dependent DnaA assembly and replication origin remodeling. *Nat. Struct. Mol. Biol.* **13,** 676–683
50. Ozaki, S., Fujimitsu, K., Kurumizaka, H., and Katayama, T. (2006) The DnaA homolog of the hyperthermophilic eubacterium *Thermotoga maritima* forms an open complex with a minimal 149-bp origin region in an ATP-dependent manner. *Genes Cells* **11,** 425–438
51. Kawakami, H., Ozaki, S., Suzuki, S., Nakamura, K., Senriuchi, T., Su'etsugu, M., Fujimitsu, K., and Katayama, T. (2006) The exceptionally tight affinity of DnaA for ATP/ADP requires a unique aspartic acid residue in the AAA+ sensor 1 motif. *Mol. Microbiol.* **62,** 1310–1324
52. Kogoma, T. (1997) Stable DNA replication. Interplay between DNA replication, homologous recombination, and transcription. *Microbiol. Mol. Biol. Rev.* **61,** 212–238
53. Stepankiw, N., Kaidow, A., Boye, E., and Bates, D. (2009) The right half of the *Escherichia coli* replication origin is not essential for viability but facilitates multiforked replication. *Mol. Microbiol.* **74,** 467–479
54. Sutton, M. D., Carr, K. M., Vicente, M., and Kaguni, J. M. (1998) *Escherichia coli* DnaA protein. The N-terminal domain and loading of DnaB helicase at the *E. coli* chromosomal origin. *J. Biol. Chem.* **273,** 34255–34262
55. Cassler, M. R., Grimwade, J. E., and Leonard, A. C. (1995) Cell cycle-specific changes in nucleoprotein complexes at a chromosomal replication origin. *EMBO J.* **14,** 5833–5841
56. Nievera, C., Torgue, J. J., Grimwade, J. E., and Leonard, A. C. (2006) SeqA blocking of DnaA-oriC interactions ensures staged assembly of the *E. coli* pre-RC. *Mol. Cell* **24,** 581–592
57. Samitt, C. E., Hansen, F. G., Miller, J. F., and Schaechter, M. (1989) *In vivo* studies of DnaA binding to the origin of replication of *Escherichia coli*. *EMBO J.* **8,** 989–993
58. Kurokawa, K., Nishida, S., Emoto, A., Sekimizu, K., and Katayama, T. (1999) Replication cycle-coordinated change of the adenine nucleotide-bound forms of DnaA protein in *Escherichia coli*. *EMBO J.* **18,** 6642–6652
59. Nishida, S., Fujimitsu, K., Sekimizu, K., Ohmura, T., Ueda, T., and Katayama, T. (2002) A nucleotide switch in the *Escherichia coli* DnaA protein initiates chromosomal replication. Evidnece from a mutant DnaA protein defective in regulatory ATP hydrolysis *in vitro* and *in vivo*. *J. Biol. Chem.* **277,** 14986–14995
60. Sauer, R. T., and Baker, T. A. (2011) AAA+ proteases. ATP-fueled machines of protein destruction. *Annu. Rev. Biochem.* **80,** 587–612
61. Glynn, S. E., Martin, A., Nager, A. R., Baker, T. A., and Sauer, R. T. (2009) Structures of asymmetric ClpX hexamers reveal nucleotide-dependent motions in an AAA+ protein-unfolding machine. *Cell* **139,** 744–756
62. Langklotz, S., Baumann, U., and Narberhaus, F. (2012) Structure and function of the bacterial AAA protease FtsH. *Biochim. Biophys. Acta* **1823,** 40–48
63. Martin, A., Baker, T. A., and Sauer, R. T. (2008) Pore loops of the AAA+ ClpX machine grip substrates to drive translocation and unfolding. *Nat. Struct. Mol. Biol.* **15,** 1147–1151
64. Aubin-Tam, M. E., Olivares, A. O., Sauer, R. T., Baker, T. A., and Lang, M. J. (2011) Single-molecule protein unfolding and translocation by an ATP-fueled proteolytic machine. *Cell* **145,** 257–267
65. Smith, D. M., Fraga, H., Reis, C., Kafri, G., and Goldberg, A. L. (2011) ATP binds to proteasomal ATPases in pairs with distinct functional effects, implying an ordered reaction cycle. *Cell* **144,** 526–538
66. Margulies, C., and Kaguni, J. M. (1996) Ordered and sequential binding of DnaA protein to oriC, the chromosomal origin of *Escherichia coli*. *J. Biol. Chem.* **271,** 17035–17040
67. Diffley, J. F. (2011) Quality control in the initiation of eukaryotic DNA replication. *Philos. Trans. R. Soc. Lond. B Biol. Sci.* **366,** 3545–3553
68. Stillman, B. (2005) Origin recognition and the chromosome cycle. *FEBS Lett.* **579,** 877–884
69. Kawakami, H., and Katayama, T. (2010) DnaA, ORC, and Cdc6. Similarity beyond the domains of life and diversity. *Biochem. Cell Biol.* **88,** 49–62
70. Clarey, M. G., Erzberger, J. P., Grob, P., Leschziner, A. E., Berger, J. M., Nogales, E., and Botchan, M. (2006) Nucleotide-dependent conformational changes in the DnaA-like core of the origin recognition complex. *Nat. Struct. Mol. Biol.* **13,** 684–690